



This discussion paper is/has been under review for the journal Natural Hazards and Earth System Sciences (NHES). Please refer to the corresponding final paper in NHES if available.

# Tephra hazard assessment at Mt. Etna (Italy)

S. Scollo<sup>1</sup>, M. Coltelli<sup>1</sup>, C. Bonadonna<sup>2</sup>, and P. Del Carlo<sup>3</sup>

<sup>1</sup>Istituto Nazionale di Geofisica e Vulcanologia, Osservatorio Etneo, Sezione di Catania, Catania, Italy

<sup>2</sup>Section des sciences de la Terre et de l'environnement, Université de Genève, Geneva, Switzerland

<sup>3</sup>Istituto Nazionale di Geofisica e Vulcanologia, Sezione di Pisa, Pisa, Italy

Received: 1 March 2013 – Accepted: 8 April 2013 – Published: 28 June 2013

Correspondence to: S. Scollo (simona.scollo@ct.ingv.it)

Published by Copernicus Publications on behalf of the European Geosciences Union.

**NHESD**

1, 2945–2981, 2013

## Tephra hazard assessment at Mt. Etna (Italy)

S. Scollo et al.

Title Page

Abstract

Introduction

Conclusions

References

Tables

Figures



Back

Close

Full Screen / Esc

Printer-friendly Version

Interactive Discussion



## Abstract

In this paper we present a probabilistic hazard assessment for tephra fallout at Mt. Etna (Italy) associated with both short- and long-lived eruptions. We analyzed wind data from the atmospheric soundings of the Italian Air Force at Trapani Birgi (western Sicily), and use the TEPHRA advection-diffusion-sedimentation model to capture the variation of wind speed and direction with time. Two different typologies of eruptions were considered in our analysis: eruptions forming strong short-lived plumes (SSL eruptions) and eruptions forming weak long-lived plumes (WLL eruptions). One Eruption Scenario (OES) for both typologies and the Eruption Range Scenario (ERS) for WLL eruptions were identified based on well documented past activity of Etna since the '90. First, model calibration was carried out for two well-known Etna explosive eruptions: the 22 July 1998 and July 2001 Etna eruptions. Second, probabilistic maps were compiled. Results clearly show that the eastern flanks are significantly affected by tephra deposition and that the WLL eruptions and the Plinian eruption of 122 BC represent the largest threat for both infrastructures and agriculture.

## 1 Introduction

Volcanic eruptions close to inhabited areas represent a major natural hazard that includes lava flows, tephra fallout, mudflows, toxic gases and other phenomena that can be triggered during the volcanic activity (e.g. tsunamis, deformation, floods, tremors). The impact of its social and economic disruption increases with respect to significant population growth (Tilling and Lipmann, 1993) and depends on the size and type of the eruption, on the prevailing wind direction and on the distance from the volcanic vent. In order to reduce risks associated with volcanic activity, careful land-use planning requires a reliable evaluation of the hazard associated with different eruptive phenomena. Among these, tephra fallout causes the collapse of buildings when the load exceeds a certain threshold and damage to agriculture, road networks and infrastructures (Blong,

**NHESSD**

1, 2945–2981, 2013

### **Tephra hazard assessment at Mt. Etna (Italy)**

S. Scollo et al.

Title Page

Abstract

Introduction

Conclusions

References

Tables

Figures

⏪

⏩

◀

▶

Back

Close

Full Screen / Esc

Printer-friendly Version

Interactive Discussion



1984; Sparks et al., 1997). In addition, fine ash produces long-term health risks such as silicosis and chronic pulmonary diseases (Horwell and Baxter, 2006) and when contaminating the atmosphere it proves extremely dangerous for air traffic. Indeed, fine ash can cause severe damage to aircraft jet engines due to both the accumulation of melted glass particles and erosion of turbine blades, interfere with electronic equipment, obstruct of the Pitot tubes that measure air speed, obscure the windscreen and landing lights and other damaging effects (Casadevall, 1994; Miller and Casadevall, 2000).

Recent studies of hazard assessment from tephra fallout have highlighted the need to combine field data of past eruptions with probabilistic approaches using well-calibrated numerical models (e.g. Barberi et al., 1990; Cioni et al., 2003; Hurst and Smith, 2004; Bonadonna et al., 2005a; Magill et al., 2006; Costa et al., 2006). While the knowledge of stratigraphic records allows characterizing the explosive activity of a given volcano and evaluating recurrence time (e.g. identification of the most probable eruptive events), numerical models of tephra dispersal help quantify the assessment of a specific phenomenon. Cioni et al. (2003) noted how the use of the simulated probability represents a significant improvement on the hazard evaluation for different volcanic phenomena and volcanic vents. Clearly, the model must be calibrated with a reliable dataset.

Although high-intensity explosive activity is rare at Etna volcano, eruptions ranging from violent strombolian to subplinian frequently occur from the summit craters and fissures can open on volcano flanks. Usually, violent strombolian activity produces weak plumes that last from several hours to months and affect the lower troposphere. As an example, between November 2002 and January 2003, a volcanic plume produced by the eruptive fracture opened on the upper SE flank of Etna at 2750 m above sea level (a.s.l.) formed a copious tephra fallout in the east part of Sicily (Andronico et al., 2005; Andronico et al., 2008). During this eruption about 80 % of crops were damaged, houses suffered structural damages and transport operations were heavily affected. Roads were covered by ash and the reduced visibility and the slipperiness caused

# NHESSD

1, 2945–2981, 2013

## Tephra hazard assessment at Mt. Etna (Italy)

S. Scollo et al.

Title Page

Abstract

Introduction

Conclusions

References

Tables

Figures

◀

▶

◀

▶

Back

Close

Full Screen / Esc

Printer-friendly Version

Interactive Discussion



several accidents (Barnard, 2004). Furthermore, airports in Catania and Reggio Calabria were forced to close for several weeks (Andronico et al., 2005). For this reason, a detailed quantification of damage due to tephra fall is necessary even for basaltic volcanoes such as Etna.

5 The reconstruction of the geological records for basaltic volcanoes is not an easy task. Thin tephra deposits are usually not preserved because they are eroded away soon after the eruptive event (hours or days). Violent strombolian activity can last several days (e.g. 2001 and 2002–2003) and its characterization is often difficult due to the high variability of eruptive phenomena and meteorological conditions that influence and scatter the fallout sedimentation (Andronico et al., 2008; Scollo et al., 2007).  
10 However, a constant monitoring of the explosive activity at Etna has been performed during the last two decades (Alparone et al., 2007; Scollo et al., 2009; Andronico et al., 2009). Many field surveys, carried out at the end of explosive activities, enabled collecting an exceptional amount of data. Some of these were used in this paper to carefully  
15 characterize the explosive activity.

We took two categories of explosive eruptions at Etna into account, the first producing strong short-lived plumes (SSL eruptions) and the latter producing weak long-lived plumes (WLL eruptions, also named Class B eruptions by Branca and Del Carlo, 2005). For each type, eruption source parameters (column height, total mass, total grain-size  
20 distribution, density of the deposit) were identified after an accurate analysis of the tephra deposits collected during the recent Etna activity. Information was also obtained by direct observations of volcanologists working at the CNR – Istituto Internazionale di Vulcanologia and the Istituto Nazionale of Geofisica e Vulcanologia, Osservatorio Etneo (INGV-OE), during the monitoring activities. In addition, we have considered the  
25 record of explosive eruptions identified within the Holocene tephrostratigraphic succession of Etna (Del Carlo et al., 2004) and the historical reports of the post-1669 AD period (Branca and Del Carlo, 2005) to include information concerning the volcanological features of Etna explosive activity. The hazard assessment has been evaluated quantitatively using the TEPHRA model (Bonadonna et al., 2005a) already applied to

# NHESSD

1, 2945–2981, 2013

## Tephra hazard assessment at Mt. Etna (Italy)

S. Scollo et al.

Title Page

Abstract

Introduction

Conclusions

References

Tables

Figures

◀

▶

◀

▶

Back

Close

Full Screen / Esc

Printer-friendly Version

Interactive Discussion



Etna (Scollo et al., 2008). The model was implemented to include the time factor necessary to model WLL eruptions. Probabilistic maps for both SSL and WLL eruptions were hence performed after model calibration for both typologies.

## 2 Etna explosive activity

5 Mt. Etna is a basaltic stratovolcano located at the front of the Apennine–Maghrebian Chain. The current activity is produced by the Mongibello volcanic center from its summit craters or lateral vents opened on volcano flanks down to a few hundred meters of altitude. Summit eruptions from the open summit craters and/or branches of the central conduits are more common than flank eruptions fed by independent paths from the central conduct (Rittmann, 1973). Although a wide variety of explosive activity does indeed take place, for many years this has been considered subordinate compared to the frequent lava flow eruptions for which Etna is generally known. The thick volcanoclastic successions that blanket the eastern slope of the Etna edifice testified important explosive activity in Late Pleistocene and Holocene times. Between 12 ka and the Present at least 25 subplinian (Branca and Del Carlo, 2005) and one plinian (in 122 BC; Coltelli et al., 1998) eruptions occurred at Etna. After the 1669 eruption, the largest and most destructive historical eruption whose eruptive vents opened at low altitude in the SE flank of the volcano (about 900 m a.s.l.), the method of observing and describing the eruptive events changed toward a more modern conception with greater detail and documented reports. The critical review of the historical reports over the last four centuries carried out by Branca and Del Carlo (2005) showed that at Etna subplinian eruptions (SSL) were produced by summit craters and lasted from a few minutes to hours, generally during periods of long-lived strombolian activity at the summit craters; nonetheless on a few occasions (e.g. 17 July 1960) they occurred during periods of quiescence. Since 1670, at least 12 subplinian eruptions have taken place (see Table 1 in Branca and Del Carlo, 2005). These events produced several kilometer-high eruptive columns that caused tephra fallout over very wide areas to distances of hundreds kilometers. On the

### Tephra hazard assessment at Mt. Etna (Italy)

S. Scollo et al.

Title Page

Abstract

Introduction

Conclusions

References

Tables

Figures

◀

▶

◀

▶

Back

Close

Full Screen / Esc

Printer-friendly Version

Interactive Discussion



contrary, the long-lived explosive activity has usually been produced by vents opened mainly on the SE flank (WLL eruptions). These kinds of eruptions produce weak eruptive plumes and proximal deposits that form large scoria cones or some coalescent cones (see Table 2 in Branca and Del Carlo, 2005). Since 1990, Etna has produced an extraordinarily high number (more than 150) of violent explosive events with fire fountains that formed eruptive columns from 5 to 15 km a.s.l. and erupted tephra volume from  $10^4$  to  $10^7$  m<sup>3</sup> (Branca and Del Carlo, 2005). These eruptions have been thoroughly described for tephra fallout dispersion and eruptive parameters (e.g. Andronico et al., 2008).

### 3 Modeling

Hazard assessment from tephra fallout is quantified using a 2-D advection-diffusion model named TEPHRA, which semi-analytically solves the mass conservation equation (see Bonadonna et al., 2005a for the model description). TEPHRA includes grain-size dependent diffusion law (Suzuki, 1983), particle density variation (Bonadonna and Phillips, 2003), stratified atmosphere (Bonadonna et al., 2002; Connor et al., 2001; Macedonio et al., 1988) and terminal settling velocity as a function of the particle Reynolds Number (Bonadonna et al., 1998). TEPHRA uses parallel computing techniques (it is written in ANSI C and uses MPI commands) suitable for the application of probabilistic approaches that require many simulations and hence are highly time-consuming. Input parameters of TEPHRA are:

- Plume Height ( $H$ ): maximum height of the eruption column determined from ground observations (e.g. Andronico et al., 2008), from satellite retrievals (e.g. Prata and Grant, 2001) and/or analysis of the field deposit (e.g. Carey and Sparks, 1986).
- Total Mass ( $M$ ): total erupted mass extrapolated from the deposit (e.g. Bonadonna and Houghton, 2005), from statistical analysis (Scollo et al., 2008) or extracted

## Tephra hazard assessment at Mt. Etna (Italy)

S. Scollo et al.

Title Page

Abstract

Introduction

Conclusions

References

Tables

Figures

◀

▶

◀

▶

Back

Close

Full Screen / Esc

Printer-friendly Version

Interactive Discussion



from empirical laws correlating the total mass with the column height (e.g. Sparks et al., 1997).

- Total Grain-size Distribution (TGS): total grain-size distribution modeled as a Gaussian distribution having a mode and standard deviation. It can be extrapolated from the tephra deposit by using different methodologies (see Bonadonna and Houghton, 2005 for a review) or estimated with a theoretical model of tephra dispersal (Mannen, 2006).
- Density of Lithics and Pumices (DL, DP): density of particles usually measured in the laboratory (e.g. Houghton and Wilson, 1989; Eychenne and Le Penneç, 2012) or using simple parameterizations (Bonadonna and Phillips, 2003).

In addition, three empirical parameters need to be evaluated through model calibration (e.g. Bonadonna et al., 2002; Scollo et al., 2007):

- Horizontal Diffusion Coefficient ( $K$ ). This parameter accounts for atmospheric diffusion and horizontal gravitation spreading of volcanic clouds. For particles having a small fall time the diffusion is regulated by Fick's law:

$$\sigma_{ij}^2 = 4K(t_{ij} + t'_i) \quad (1)$$

where  $i$  is for the point sources along the eruptive plume,  $j$  is the particle size,  $K$  ( $\text{m}^2 \text{s}^{-1}$ ) is the atmospheric horizontal diffusion coefficient,  $t_{ij}$  (s) is fall time of a particle of size  $j$  released from a point source  $i$  along the eruptive plume and  $t'_i$  (s) is the horizontal diffusion time in the vertical plume, which accounts for the change in width of the vertical plume with height (Ernst et al., 1996; Woods, 1995; Morton et al., 1956; Sparks and Wilson, 1982; Bonadonna et al., 2005). For particle fall time with a scale of hours the diffusion is described by a power law (Suzuki, 1983):

$$\sigma_{ij}^2 = \frac{8C}{5}(t_{ij} + t'_i)^{2.5} \quad (2)$$

## NHESSD

1, 2945–2981, 2013

### Tephra hazard assessment at Mt. Etna (Italy)

S. Scollo et al.

Title Page

Abstract

Introduction

Conclusions

References

Tables

Figures

◀

▶

◀

▶

Back

Close

Full Screen / Esc

Printer-friendly Version

Interactive Discussion



where  $C$  is the apparent eddy diffusivity determined empirically with  $C = 0.04 \text{ m}^2 \text{ s}^{-1}$  (Suzuki, 1983).

- Fall Time Threshold (FTT): parameter that indicates the shift between Fickian and power-law diffusion. Larger values of FTT mean that more particles follow the linear diffusion, and therefore produce a thick and narrow deposit in the proximal area centered along the dispersal axis.
- Plume Ratio (PR): parameter related to the plume mass distribution. The mass of erupted tephra is assumed to be uniformly distributed with height but there is the option of choosing where the mass is mainly located (i.e. ratio between total height and the lower plume level where particles start being released).

### 3.1 Model Implementation

Semi-analytical tephra dispersal models assume that volcanic particles are instantaneously released at the time zero (e.g. TEPHRA, Bonadonna et al., 2005a; HAZMAP, Barberi et al., 1990; Macedonio et al., 2005; ASHFALL, Hurst and Turner, 1999). They are usually applied to relatively short-lived activity such as subplinian and plinian eruptions (Suzuki, 1983; Armienti et al., 1988; Hurst and Turner, 1999; Connor et al., 2001). Nevertheless, violent strombolian eruptions, such as the 2001 and 2002–2003 Etna eruptions, can last several days (Scollo et al., 2007; Andronico et al., 2008) and are significantly affected by wind variations (Bursik et al., 1992; Sparks et al., 1997). TEPHRA was hence implemented to account for the variation in wind direction and speed with time in order to compile a comprehensive hazard assessment of WLL eruptions. In particular, a specific number of wind profiles,  $n$ , associated with a given eruption is determined by dividing the total eruption duration by the interval between available wind profiles (e.g. six hours for the atmospheric sounding data of the Italian Air Force (IAF) at Trapani Birgi, (located in western Sicily) used in our analysis). For instance, if the total eruption duration is 84 h, the number of wind profiles  $n$  is 14. When the duration cannot be divided by the time interval (6 h) the number of wind profile is approximated.

## Tephra hazard assessment at Mt. Etna (Italy)

S. Scollo et al.

Title Page

Abstract

Introduction

Conclusions

References

Tables

Figures

◀

▶

◀

▶

Back

Close

Full Screen / Esc

Printer-friendly Version

Interactive Discussion



The total erupted mass is then divided by  $n$ , and  $n$  eruptions of mass of  $M/n$  are sequentially run assuming constant eruptive parameters (i.e.  $H$ , TGS, DL and DP, PR,  $K$ , FTT). The fraction  $m_{i,j}$  of particles with size  $j$  that fall from a point source  $i$  at a point on the ground with coordinates  $(x,y)$  is determined as the sum of the contribution of the  $n$  eruptions of mass  $M/n$ :

$$m_{i,j}(x,y) = \sum_{s=1}^n m_{i,j}(x,y) \quad (3)$$

where  $s$  indicates the simulations between 1 and  $n$ .

#### 4 Model calibration

TEPHRA is calibrated by varying empirical parameters ( $K$ , FTT and PR) and finding the best fit between computed and observed data by the minimum of the  $mf$  function (Bonadonna et al., 2002):

$$mf = \sqrt{\frac{\sum (M_{\text{obs}} - M_{\text{comp}})^2}{N - 1}} \quad (4)$$

where  $N$  is the number of field data,  $M_{\text{obs}}$  ( $\text{kg m}^{-2}$ ) and  $M_{\text{comp}}$  ( $\text{kg m}^{-2}$ ) are the observed and computed masses accumulated per area unit. The calibration was carried out for SSL and WLL eruptions. In detail, the SSL calibration is based on the 22 July 1998 eruption (Aloisi et al., 2002; Andronico et al., 1999; Scollo et al., 2008) and the WLL calibration on the 21–24 July phase of the 2001 eruption (Scollo et al., 2007).

##### 4.1 Model calibration for eruptions generating strong short-lived plumes

Calibration of the SSL eruptions was based on data collected after the activity of 22 July 1998, one of the largest events to occur at Etna since the last century

## Tephra hazard assessment at Mt. Etna (Italy)

S. Scollo et al.

Title Page

Abstract

Introduction

Conclusions

References

Tables

Figures

◀

▶

◀

▶

Back

Close

Full Screen / Esc

Printer-friendly Version

Interactive Discussion



(Andronico et al., 1999). A sustained column reached an altitude of 12 km (a.s.l.) forming a typical strong plume (Fig. 1a). The wind direction was almost constant, about 140° from the north, up to 10 km where it began to blow toward NE (about 50° from the north) and with an intensity of less than 10 m s<sup>-1</sup> (Aloisi et al., 2002). The eruption produced an abundant tephra fallout deposit on the south-eastern flank. Thirty-five samples were collected a few hours after the end of the eruptive episode; from the analysis of the tephra deposit the eruption was classified subplinian (Andronico et al., 1999). The total mass of pyroclastic material erupted was estimated using Pyle's method (1989) about 1.3 × 10<sup>9</sup> kg (Andronico et al., 1999) and the total grain-size distribution was centered on 2 ϕ with a standard deviation of 1.5 (Scollo et al., 2008) using Voronoi's method (Bonadonna and Houghton, 2005). Model calibration was carried out varying *K* between 0.001 and 6800 m<sup>2</sup> s<sup>-1</sup>, FTT between 36 and 3600 s and PR between 0 and 1. The best-fit values were obtained for *K* equals to 200 m<sup>2</sup> s<sup>-1</sup>, FTT equals to 180 sec (i.e. 0.05 h) and PR equals to 0.4 (Fig. 2a, b and c). On the basis of these values, a new simulation was performed and local differences among the computed best fit values and the field data were evaluated at each sampling point (Fig. 2d). The largest discrepancies are shown by locations with mass accumulation >10 kg m<sup>-2</sup>. Finally, the comparisons among the grain-size distributions of the samples and those computed at the same locations show a good agreement at different distances from the vent (Fig. 3).

#### 4.2 Model calibration for eruptions generating weak long-lived plumes

The WLL calibration was based on data collected after the first phreatomagmatic phase of 2001 Etna eruption between 21 and 24 July (Fig. 1b), already used for validating several models (Scollo et al., 2007; Costa et al., 2006; Barsotti et al., 2008). During this event, a weak and long-lived plume rose up to 5 km of altitude from a vent opened at 2570 m a.s.l. on SE flank of Etna. The deposit was bilobate in shape due to the change of explosive intensity and wind direction and velocity. It covered the area between Giarre and Catania with two dispersal axes toward S and SSE. From the analysis of 46 samples, a total volume of 2.32 × 10<sup>9</sup> kg and a total grain-size distribution of 2 ϕ

## Tephra hazard assessment at Mt. Etna (Italy)

S. Scollo et al.

Title Page

Abstract

Introduction

Conclusions

References

Tables

Figures

◀

▶

◀

▶

Back

Close

Full Screen / Esc

Printer-friendly Version

Interactive Discussion



were calculated by using the power law and Voronoi's methods, respectively (Scollo et al., 2007).

Like the SSL eruption calibration,  $K$  was changed between 0.001 and 6800 m<sup>2</sup> s<sup>-1</sup>, FTT between 36 and 10 800 s PR between 0 and 1 (Fig. 4a, b and c). Best-fit values were obtained for  $K$  equals to 1800 m<sup>2</sup> s<sup>-1</sup>, FTT equals to 2520 s (i.e., 0.7 h) and PR equals to 1. The agreement between computed and field data is shown in Fig. 4d, while the comparison between grain-size distributions of the collected samples and grain-size distributions computed at the same locations is shown in Fig. 5.

## 5 Wind data analysis

We analyzed wind data taken from atmospheric soundings by the IAF from January 1990 to 2003. Data were converted in a compatible format for the TEPHRA model that requires the direction (degree calculated from the north of provenance +180°) and wind speed (m s<sup>-1</sup>) from 1 to 30 km of altitude, by 1 km step. Winds usually blow to the south east in the lower troposphere, moving toward east as altitude increases (Fig. 6a). The mean direction of the wind is between 97° and 173° (provenance of the wind +180°) with a standard deviation between 38° and 93°. The mean speed is roughly between 7 and 23 m s<sup>-1</sup> with a standard deviation between 4 and 11 m s<sup>-1</sup> (Fig. 6b). The wind speed increases regularly in the troposphere up to 11 km of altitude (going up to 25 m s<sup>-1</sup>) and decreases at the tropopause, dropping regularly to 8.5 m s<sup>-1</sup> at 20 km of altitude (Fig. 6b). Plotting wind directions for different altitudes (5, 10, 15 and 20 km) in Fig. 7, we may evaluate its maximum probability that is mainly between 90 and 120°.

## 6 Hazard assessment

In our analysis we have compiled probability maps for:

# NHESSD

1, 2945–2981, 2013

## Tephra hazard assessment at Mt. Etna (Italy)

S. Scollo et al.

Title Page

Abstract

Introduction

Conclusions

References

Tables

Figures

◀

▶

◀

▶

Back

Close

Full Screen / Esc

Printer-friendly Version

Interactive Discussion



## Tephra hazard assessment at Mt. Etna (Italy)

S. Scollo et al.

Title Page

Abstract

Introduction

Conclusions

References

Tables

Figures

◀

▶

◀

▶

Back

Close

Full Screen / Esc

Printer-friendly Version

Interactive Discussion



- One Eruption Scenario of SSL eruption. We compiled probability maps based on two large explosive events of Etna volcano: (i) the 1990 eruption, the largest eruptive event in the last three centuries; category 1 (OES-SSL1) and (ii) the Plinian eruption of 122 BC, the largest eruptive event occurring in last 12 000 yr; category 2 (OES-SSL2).
- One Eruption Scenario of WLL eruption (OES-WLL). We compiled probability maps based on the 2002–2003 eruption.
- Eruption Range Scenarios of WLL eruption (ERS-WLL). We compiled probability maps based on WLL eruptions recorded in the last three centuries.

OES and ERS are described in Bonadonna (2006). We also considered the following hazardous thresholds: (i) roof collapse ( $100, 200$  and  $300 \text{ kg m}^{-2}$ ; Cioni et al., 2003) and (ii) damage to vegetation ( $10 \text{ kg m}^{-2}$ ; Bonadonna et al., 2005a).

### 6.1 One Eruption Scenario probability maps associated with strong short-lived plumes (category 1)

The eruption of 5 January 1990 was the largest explosive event of the last 300 yr and represents our case study for eruptions generating strong short-lived plumes (category 1). It began at 03:00 UTC from the South East Crater and lasted for about 35 min (Calvari et al., 1991; Carveni et al., 1994). Unfortunately, there were very few direct observations due to adverse atmospheric conditions but some samples were collected a few days after the event allowing classifying this eruption as subplinian (Calvari et al., 1991). The pyroclastic deposit covered almost the whole of the WNW Etna flank. The proximal deposit was made up of light spatter bombs and lapilli having a clast density of  $1160 \text{ kg m}^{-3}$ . A 4 m and 9 cm thick deposit was found at 0.5 and 6.5 km downwind from the volcanic vent, respectively (Calvari et al., 1991). The morphoscopic analysis revealed the most abundant fragments were highly vesiculated with surfaces bounded by bubble walls or by concoidal fractures (Calvari et al., 1991). Given that more physical



was found in the Ionian sea at 400 km from the vents. During the Plinian phase (C and E units) a total volume of  $0.285 \text{ km}^3$  was erupted, and the column height reached 24–26 km a.s.l. (Coltelli et al., 1998). Probability maps for this event show that the tephra accumulation has a very high probability (between 50–100 %) of exceeding  $100 \text{ kg m}^{-2}$  up to about 30 km from the volcanic vent (Fig. 10). There is also a 20 % of probability of exceeding  $300 \text{ kg m}^{-2}$  within 15 km from the volcanic vent. Roof collapses may occur in large densely populated areas such as Giarre and Zafferana towns (between 40 % and 70 % for 300 and  $100 \text{ kg m}^{-2}$ , respectively).

### 6.3 One Eruption Scenario probability maps associated with weak long-lived plumes

The eruption of 2002–2003 was used to compile the OES-WLL probability maps. This eruption began on 26 October 2002 with the opening of a complex system of eruptive fissures on the north east (from 3010 to 2920 m and from 2500 to 1890 m) and south (from 2850 to 2600 m) flanks. The eruption ended on 28 January 2003, after three months of almost continuous explosive activity and lava flow emission. Tall eruption columns up to 7 km a.s.l., were emitted from the S fissure continuously for 56 days. Abundant tephra falls on all the volcano's flanks, often forcing the closure of the airports in Catania and Reggio Calabria (Andronico et al., 2005). Lapilli and ash mainly covered the E sectors of the volcano due to dominant winds that blew eastward. A total volume of  $43 \times 10^6 \text{ m}^3$  and a total grain-size distribution peaked at  $0.5 \phi$  was estimated by Andronico et al. (2008). Over the past three centuries, this activity has been considered comparable only with the 1763 eruption (Andronico et al., 2005) that was produced from La Montagnola volcanic cone located near the 2002–2003 vent and lasting 84 days (Recupero, 1815).

The OES-WLL probability maps were compiled considering an eruption lasting for 100 days and producing a weak plume of 7 km a.s.l (Fig. 11). Tephra accumulation has a very high probability (between 80–100 %) of exceeding 300, 200 and  $100 \text{ kg m}^{-2}$

## Tephra hazard assessment at Mt. Etna (Italy)

S. Scollo et al.

Title Page

Abstract

Introduction

Conclusions

References

Tables

Figures

◀

▶

◀

▶

Back

Close

Full Screen / Esc

Printer-friendly Version

Interactive Discussion



within 6, 12 and 18 km from the vent, respectively and affected mainly the south-eastern flanks of volcano.

#### 6.4 Eruption Range Scenario probability maps associated with weak long-lived plumes

5 Eruption Range Scenario was evaluated for WLL eruptions because only for this case we may consider a future prolonged multi-vent activity. From the analysis carried out by Branca and Del Carlo (2005), we consider the column heights variable between 3.6 km and 7 km a.s.l. (Fig. 12). The duration of the eruption was assumed between 4 (2001 Etna eruption) and 100 days (Fig. 13). Volcanic vents were taken randomly (Fig. 14a) and their locations (latitude, longitude and height) were also sampled statistically for the hazard assessment. Probability maps are shown in Fig. 14b, c and d. For a threshold of  $300 \text{ kg m}^{-2}$  there is a small probability (between 1–20 %) that the mass exceeds this loading behind 15 km, and between 10 and 20 % occur between 10 and 15 km. Instead, considering a threshold of  $200 \text{ kg m}^{-2}$  the probability that the mass exceeds this loading is between 1 and 30 % within 20 km. Finally, for a threshold of  $100 \text{ kg m}^{-2}$  the probability  $>20 \%$  occurs at distances  $<20 \text{ km}$ .

## 7 Discussion

The evaluation of eruption source parameters is necessary to reliably model volcanic ash transport during an eruption (Mastin et al., 2009) and to calibrate and validate volcanic ash transport and dispersion models (Scollo et al., 2008). This is why the IAVCEI Commission on Tephra Hazard Modelling makes a comprehensive dataset (<http://dbstr.ct.ingv.it/iavcei/>) available in order to improve model reliability by comparisons among data and model results. While detailed field observations are necessary to characterize the explosive activity, numerical models represent a powerful tool to quantitatively analyze the effects caused by the eruption. Over the last 30 yr, increasingly

## Tephra hazard assessment at Mt. Etna (Italy)

S. Scollo et al.

Title Page

Abstract

Introduction

Conclusions

References

Tables

Figures

◀

▶

◀

▶

Back

Close

Full Screen / Esc

Printer-friendly Version

Interactive Discussion



## Tephra hazard assessment at Mt. Etna (Italy)

S. Scollo et al.

Title Page

Abstract

Introduction

Conclusions

References

Tables

Figures

◀

▶

◀

▶

Back

Close

Full Screen / Esc

Printer-friendly Version

Interactive Discussion



sophisticated numerical models have greatly helped represent the natural system realistically (Sheridan, 1994; Costa and Macedonio, 2005; Ongaro et al., 2012). To evaluate the impact from tephra fallout, the last generation of models takes full advantage of parallel programming (Wilkinson and Allen, 1999), which has enabled improving physical models and using probabilistic analysis with greater accuracy (e.g. Bonadonna et al., 2005a; Neri et al., 2007; Folch et al., 2008).

TEPHRA and the whole generation of semi-analytical models is based on the assumption that both the particle release occurs at time  $t = 0$ . As a result, these models cannot capture the variation of wind velocity and direction with time and have been typically used for the hazard assessment of strong and relatively short-lived eruptions. By contrast, the implementation of the TEPHRA model has allowed the compilation of probability maps also for long-lived eruptions and consequently results may be compared with those obtained by other models that instead consider the time variability of the eruption (e.g. FALL3D and VOLCALPUFF, in Costa et al., 2006 and Barsotti et al., 2008).

It should be noted, for SSL eruptions, that TEPHRA does not reproduce the deposit well within the plume corner. The greatest differences among the model and field data are in fact located between 1.8 and 3.8 km from the vent. Instead, for WLL eruptions (the 21–24 July 2001 Etna eruption) TEPHRA gives higher values than those observed in the distal region. This could depend on the fact that very thin deposits might not be preserved in distal region (Bonadonna et al., 2002; Scollo et al., 2007). Nevertheless, it is notable that the best fit between the computed and the field data is still good (within 50%) and consequently we can assert that TEPHRA may provide a reliable hazard assessment.

In our study we considered and calibrated the TEPHRA model for weak- and strong-plume typologies. For strong plumes, the plume vertical velocity is greater than the wind speed, whereas for weak plumes it is lower than wind speed (Carey and Sparks, 1986). The spreading umbrella cloud of strong plumes can be described as turbulent currents, while weak plumes develop bent-over trajectories that are typically identified

## Tephra hazard assessment at Mt. Etna (Italy)

S. Scollo et al.

Title Page

Abstract

Introduction

Conclusions

References

Tables

Figures

◀

▶

◀

▶

Back

Close

Full Screen / Esc

Printer-friendly Version

Interactive Discussion



by empirical curve fitting (Sparks et al., 1997). Moreover, in a strong plume, sedimentation processes are mainly generated from the umbrella region that gives the greatest contribution to the total tephra-fallout (Sparks et al., 1997; Bonadonna and Phillips, 2003). In a weak plume, on the other hand, wind significantly affects the current spreading and particle sedimentation, resulting in particle depletion within proximal areas and enhanced accumulation in distal areas. As a result, plume-corner mass accumulation and transition of fallout regimes are shifted downwind (Bonadonna et al., 2005b). Finally, weak plumes may also bifurcate in distal areas probably due to the distribution of pressure around the vortices, constant plume buoyancy, and release of latent heat by evaporating water droplets within the plume (Ernst et al., 1996).

The results of the hazard assessment at Etna have indicated that deposits associated with OES-WLL eruptions are very dangerous. Probability maps have shown mass accumulation  $\geq 200$  and  $\geq 100 \text{ kg m}^{-2}$  can be reached within 18 and 23 km from the vent. Densely populated cities, located in the eastern flank of the volcano such as Acireale and Giarre, can be seriously affected by OES-WLL eruptions. This is in agreement with the results obtained by Barsotti et al. (2010), that showed that towns and infrastructures on the east side of the volcano are significantly more exposed to ash hazard. These towns may therefore be severely affected by the tephra fallout and cleanup of roofs and roads is hence required to prevent disasters.

We found that Catania could be affected by OES-WLL eruptions even if the probability of reaching a threshold of  $100 \text{ kg m}^{-2}$  is relatively low (between 10 and 30 %). On the contrary, OES-SSL1 seems to produce only damage to agriculture. ERS-WLL has minor effects than OES-SSL1, but they should not be underrated. Indeed, there is the probability (even if low) that the accumulation of  $100 \text{ kg m}^{-2}$  can be reached in densely populated areas. Finally, in the case of an exceptional event like a basaltic Plinian eruption (OES-SSL2 scenario), there is a very high probability that roof collapses may happen in all areas around the volcano within 50 km from the vent. It is highlighted that, respect to previous works on probabilistic hazard assessment for tephra fallout at Mt Etna, we evaluated for the first time probability maps using standard thresholds for roof

collapses and damage to vegetation. Moreover, the 5 January 1990 event that may be considered as the most explosive event of the last 300 yr and the 122 BC Plinian eruption were analyzed in detail in order to estimate reliable eruption source parameters. For these events, the use of probabilities maps allows us to evaluate, for the first time, their impact in inhabited areas nearby Etna.

## 8 Conclusive remarks

In this work, a detailed hazard assessment was carried out on the basis of two different typologies of Etna eruptions: eruptions associated with strong short-lived plumes (SSL eruptions) and eruptions associated with weak long-lived plumes (WLL eruptions). Among them, the most powerful eruptive activities have been identified. We chose four different scenarios and prolonged multi-event activity to take account of the great variability that may occur at basaltic volcanoes such as Etna. Results clearly show that the east flank is strongly affected, largely owing to the wind direction. In particular, eruptions such as the 2002–2003 and 122 BC Plinian eruptions, never considered before, are the most dangerous with the highest probability of roof collapse. However, severe damage to agriculture occurs on the east side of volcano for all the different eruption types considered in our study. Future research could include more eruptive scenarios, such as the recent lava fountaining activity in 2011 and 2012, as well as different volcanic ash dispersal models (e.g. lagrangian and eulerian models).

*Acknowledgements.* The authors are grateful to Istituto Nazionale di Geofisica e Vulcanologia and to the University of Hawaii for supporting this project. We are also grateful to L. Connor for her advice on the TEPHRA implementation carried out in this work, to F. Rapicavoli for the help given during the analysis of wind data, D. Andronico for allowing us to use field data collected during the 1998 Etna eruption, and G. Spata for his support. This work was supported by INGV-GNV fellowship and MIUR-FIRB Italian project “Sviluppo Nuove Tecnologie per la Protezione e Difesa del Territorio dai Rischi Naturali for one of the authors (S. Scollo). The native English speaker Stephen Conway is sincerely thanked.

### Tephra hazard assessment at Mt. Etna (Italy)

S. Scollo et al.

Title Page

Abstract

Introduction

Conclusions

References

Tables

Figures

◀

▶

◀

▶

Back

Close

Full Screen / Esc

Printer-friendly Version

Interactive Discussion



## References

- Aloisi, M., D'Agostino, M., Dean, K., G., Mostaccio, A., and Neri, G.: Satellite analysis and PUFF simulation of the eruptive cloud generated by the Mount Etna paroxysm of 22 July 1998, *J. Geophys. Res.*, 107, doi:10.1029/2001JB000630, 2002.
- 5 Alparone, S., Andronico, D., Sgroi, T., Ferrari, F., Lodato, L., and Reitano, D.: Alert system to mitigate tephra fallout hazards at Mt. Etna Volcano, Italy, *Nat. Hazards*, 43, 333–350, 2007.
- Andronico, D., Del Carlo, P., and Coltelli, M.: The 22 July 1998 fire fountain episode at Voragine Crater (Mt Etna, Italy), *Volcanic and Magmatic Studies Group, Annual Meeting*, 5–6 January 1999, Birmingham, 1999.
- 10 Andronico, D., Branca, S., Calvari, S., Burton, M.R., Caltabiano, T., Corsaro, R.A., Del Carlo, P., Garfi, G., Lodato, L., Miraglia, L., Murè, F., Neri, M., Pecora, E., Pompilio, M., Salerno, G., and Spampinato, L., 2005: A multi-disciplinary study of the 2002–03 Etna eruption: Insights for a complex plumbing system, *Bull. Volcanol.*, 67, 314–330, 2005.
- Andronico, D., Scollo, S., Cristaldi A., and Caruso, S.: The 2002–03 Etna explosive activity: tephra dispersal and features of the deposit, *J. Geophys. Res.*, 113, B04209, doi:10.1029/2007JB005126, 2008.
- 15 Andronico, D., Scollo, S., Cristaldi, A., and Ferrari, F.: Monitoring the ash emission episodes at Mt. Etna: the 16 November 2006 case study, *J. Volcanol. Geotherm. Res.*, 180, 123–134, 2009.
- 20 Armienti, P., Macedonio, G., and Pareschi, M. T.: A numerical-model for simulation of tephra transport and deposition-applications to May 18 1980, Mount St-Helens eruption, *J. Volcanol. Geotherm. Res.*, 93, 6463–6476, 1988.
- Barberi, F., Macedonio, G., Pareschi, M. T., and Santacroce, R.: Mapping the tephra fallout risk: an example from Vesuvius, Italy, *Nature*, 344, 142–144, 1990.
- 25 Barnard, S. T.: Results of a reconnaissance trip to Mt. Etna, Italy: The effects of the 2002 eruption of Etna on the province of Catania, *Bull. New Zealand Soc. Earthquake Eng.*, 37, 47–62, 2004.
- Barsotti, S., Neri, A., and Scire, J. S.: The Vol-CALPUFF model for atmospheric ash dispersal: I Approach and physical formulation, *J. Geophys. Res.*, 113, B03208, doi:10.1029/2006JB004623, 2008.
- 30

## Tephra hazard assessment at Mt. Etna (Italy)

S. Scollo et al.

Title Page

Abstract

Introduction

Conclusions

References

Tables

Figures

◀

▶

◀

▶

Back

Close

Full Screen / Esc

Printer-friendly Version

Interactive Discussion



**Tephra hazard  
assessment at Mt.  
Etna (Italy)**

S. Scollo et al.

Title Page

Abstract

Introduction

Conclusions

References

Tables

Figures

◀

▶

◀

▶

Back

Close

Full Screen / Esc

Printer-friendly Version

Interactive Discussion



- Barsotti, S., Andronico, D., Neri, A., Del Carlo, P., Baxter, P. J., Aspinall, W. P., and Hincks, T.: Quantitative assessment of volcanic ash hazards for health and infrastructure at Mt. Etna (Italy) by numerical simulation, *J. Volcanol. Geotherm. Res.*, 192, 85–96, 2010.
- Blong, R. J.: *Volcanic Hazards. A sourcebook on the effects of eruptions*, Academic Press, Sidney, 1984.
- Bonadonna, C.: Probabilistic modelling of tephra dispersal, in: *Statistics in Volcanology*, edited by: Mader, H., Cole, S., and Connor, C. B., IAVCEI Series Volume 1, Geological Society of London, 2006.
- Bonadonna, C., and Houghton, B. F.: Total grain-size distribution and volume of tephra-fallout deposits, *Bull. Volcanol.*, 67, 441–456, 2005.
- Bonadonna, C. and Phillips, J. C.: Sedimentation from strong volcanic plumes, *J. Geophys. Res.*, 108, 2340, doi:10.1029/2002JB002034, 2003.
- Bonadonna, C., Ernst, G. G. J., and Sparks, R. S. J.: Thickness variations and volume estimates of tephra fall deposits: the importance of particle Reynolds number, *J. Volcanol. Geotherm. Res.*, 81, 173–187, 1998.
- Bonadonna, C., Macedonio, G., and Sparks, R. S. J.: Numerical modelling of tephra fallout associated with dome collapses and Vulcanian explosions: application to hazard assessment on Montserrat, Geological Society, London, Memoir, 2002.
- Bonadonna, C., Connor, C. B., Houghton, B. F., Sahetapy-Engel, S., Hincks, T., and Connor, L.: Probabilistic modelling of tephra dispersion: Hazard assessment of a multi-phase rhyolitic eruption at Tarawera, New Zealand, *J. Geophys. Res.*, 110, B03203, doi:10.1029/2003JB002896, 2005a.
- Bonadonna, C., Phillips, J. C., and Houghton, B. F.: Modelling tephra sedimentation from a Ruapeho weak plume eruption, *J. Geophys. Res.*, 110, B08209, doi:10.1029/2004JB003515, 2005b.
- Branca, S. and Del Carlo, P.: Types of eruptions of Etna Volcano AD 1670–2003: Implications for short-term eruptive behaviour, *Bull. Volcanol.*, 67, 732–742, 2005.
- Bursik, M. I., Carey, S. N., and Sparks, R. S. J.: A gravity current model for the May 18, 1980 Mount-St-Helens plume, *Geophys. Res. Lett.*, 19, 1663–1666, 1992.
- Calvari, S., Coltelli, M., Pompilio, M., and Scrivano, V.: The eruptive activity between October 1989 and December 1990, *Acta Vulcanol.*, 1, 257–260, 1991.
- Carey, S. N. and Sparks, R. S. J.: Quantitative models of the fallout and dispersal of tephra from volcanic eruption columns, *Bull. Volcanol.*, 48, 109–125, 1986.

## Tephra hazard assessment at Mt. Etna (Italy)

S. Scollo et al.

Title Page

Abstract

Introduction

Conclusions

References

Tables

Figures

◀

▶

◀

▶

Back

Close

Full Screen / Esc

Printer-friendly Version

Interactive Discussion



- Carveni, P., Romano, R., Caltabiano, T., Grasso, M. F., and Gresta, S.: The exceptional explosive activity of 5 January 1990 at SE-Crater of Mt Etna volcano (Sicily), *Boll. Soc. Geol. It.*, 113, 613–631, 1994.
- Casadevall, T. J.: Volcanic Ash and Aviation Safety: Proceedings of the First International Symposium on Volcanic Ash and Aviation Safety, US Geological Survey Bulletin, vol. 2047, 1994.
- Cioni, R., Longo, A., Macedonio, G., Santacroce, R., Sbrana, A., Sulpizio, R., and Andronico, D.: Assessing pyroclastic fall hazard through field data and numerical simulations: Example from Vesuvio, *J. Geophys. Res.*, 108, 2063, doi:10.1029/2001JB000642, 2003.
- Coltelli, M., Del Carlo, P., and Vezzoli, L.: The discovery of a Plinian basaltic eruption of Roman age at Mt. Etna, *Geology*, 26, 1095–1098, 1998.
- Connor, C. B., Hill, B. E., Winfrey, B., Franklin, N. M., and La Femina P. C.: Estimation of volcanic hazards from tephra fallout, *Nat. Hazards Rev.*, 2, 33–42, 2001.
- Costa, A. and Macedonio G.: Numerical simulation of lava flows based on depth-averaged equations, *Geophys. Res. Lett.*, 32, L05304, doi:10.1029/2004GL021817, 2005.
- Costa, A., Macedonio, G., and Folch, A.: A three dimensional Eulerian model for transport and deposition of volcanic ashes, *Earth Planet. Sci. Lett.*, 241, 634–647, 2006.
- Del Carlo, P., Vezzoli, L., and Coltelli, M.: Last 100 ka tephrostratigraphic record of Mount Etna, edited by: Bonaccorso, A., Calvari, S., Coltelli, M., Del Negro, C., and Falsaperla, S., AGU Geophysical Monograph Series volume, 2004.
- Ernst, G. G. J., Sparks, R. S. J., Carey, S. N., and Bursik, M. I.: Sedimentation from turbulent jets and plumes, *J. Geophys. Res.*, 101, 5575–5589, 1996.
- Eychenne, J. and Le Pennec, J. L.: Sigmoidal particle density distribution in a subplinian scoria fall deposit, *Bull. Volcanol.*, 74, 2243–2249, 2012.
- Folch, A., Cavazzoni, C., Costa, A., and Macedonio, G.: An automatic procedure to forecast tephra fallout, *J. Volcanol. Geotherm. Res.*, 177, 767–777, 2008.
- Horwell, C. J. and Baxter, P. J.: The respiratory health hazards of volcanic ash: a review for volcanic risk mitigation, *Bull. Volcanol.*, 69, 1–24, 2006.
- Houghton, B. F. and Wilson, C. J. N.: A vesicularity index for pyroclastic deposits, *Bull. Volcanol.*, 51, 451–462, 1989.
- Hurst, T. and Smith, W.: A Monte Carlo methodology for modeling ashfall hazards, *J. Volcanol. Geotherm. Res.*, 138, 393–403, 2004.



**Tephra hazard  
assessment at Mt.  
Etna (Italy)**

S. Scollo et al.

Title Page

Abstract

Introduction

Conclusions

References

Tables

Figures

◀

▶

◀

▶

Back

Close

Full Screen / Esc

Printer-friendly Version

Interactive Discussion



Scollo, S., Tarantola, S., Bonadonna, C., Coltelli, M., and Saltelli, A.: Sensitivity analysis and uncertainty estimation for tephra dispersal models, *J. Geophys. Res.*, 113, B06202, doi:10.1029/2006JB004864, 2008.

5 Scollo, S., Prestifilippo, M., Spata, G., D'Agostino, M., and Coltelli, M.: Monitoring and forecasting Etna volcanic plumes, *Nat. Hazards Earth Syst. Sci.*, 9, 1573–1585, doi:10.5194/nhess-9-1573-2009, 2009.

Sheridan, M. F.: Volcanology – from model to reality, *Nature*, 367, p. 514, 1994.

10 Sparks, R. S. J. and Wilson, L.: Explosive volcanic eruptions: V. Observations of plume dynamics during the 1979 Soufrière eruption, St. Vincent, *Geophys. J. Roy. Astr. S.*, 69, 551–570, 1982.

Sparks, R. S. J., Bursik, M. I., Carey, S. N., Gilbert, J. S., Glaze, L. S., Sigurdsson, H., and Woods, A. W.: John Wiley & Sons, Chichester, *Volcanic Plumes*, 1997.

Suzuki, T.: A theoretical model for dispersion of tephra, *Arc Volcanism, Physics and Tectonics*, Terra Scientific Publishing Company Terrapub, Tokyo, 1983.

15 Tilling, R. I. and Lipman, P. W.: Lessons in reducing volcano risk, *Nature*, 364, 277–280, 1993.

Wilkinson, B. and Allen, M.: *Parallel Programming: Techniques and Applications Using Networked Workstations and Parallel Computers*, Prentice-Hall, 1999.

Woods, W.: The dynamics of explosive volcanic eruptions, *Rev. Geophys.*, 33, 495–530, 1995.

**Tephra hazard  
assessment at Mt.  
Etna (Italy)**

S. Scollo et al.

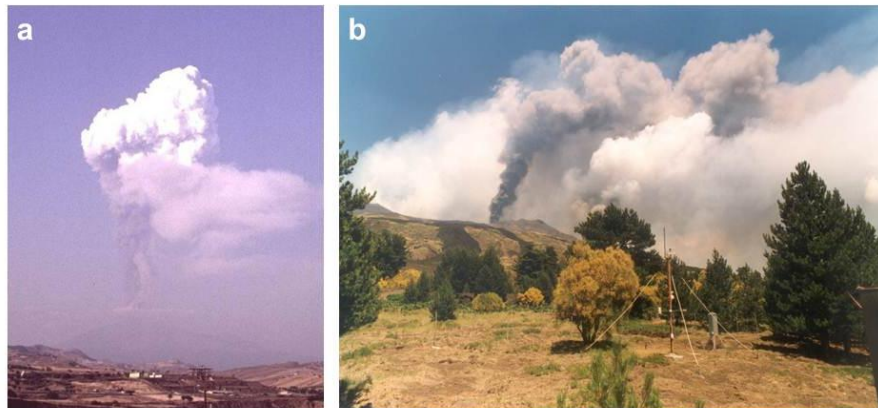


**Fig. 1.** Examples of **(a)** SSL plume produced during 22 July 1998 Etna eruption (courtesy of M. Pompilio); **(b)** WLL plume formed on 24 July 2001 (photo taken by S. Scollo).

[Title Page](#)[Abstract](#)[Introduction](#)[Conclusions](#)[References](#)[Tables](#)[Figures](#)[◀](#)[▶](#)[◀](#)[▶](#)[Back](#)[Close](#)[Full Screen / Esc](#)[Printer-friendly Version](#)[Interactive Discussion](#)

## Tephra hazard assessment at Mt. Etna (Italy)

S. Scollo et al.

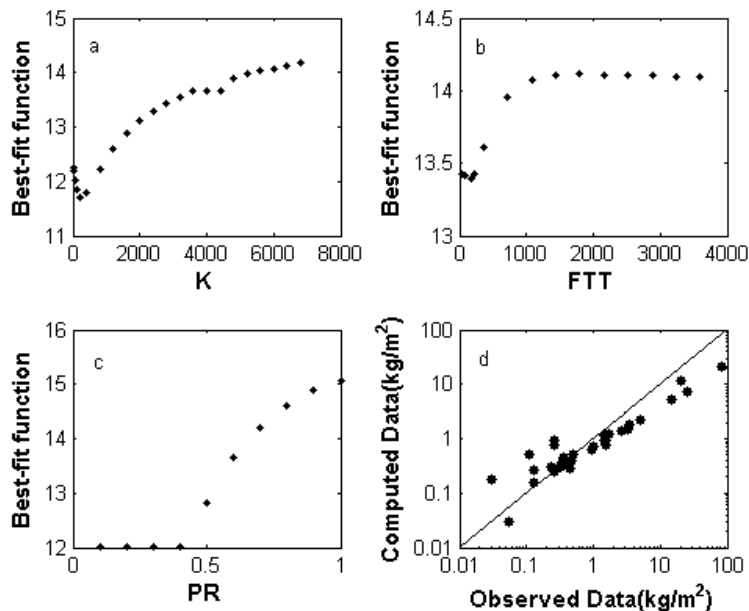


**Fig. 2.** Misfit function calculated varying: **(a)** the atmospheric horizontal diffusion coefficient ( $K$ ) between  $0.001$ – $6800 \text{ m}^2 \text{ s}^{-1}$ ; **(b)** the Fall Time Threshold (FTT) between  $36$ – $3600 \text{ s}$  and **(c)** the Plume Ratio (PR) between  $0$ – $1$ ; **(d)** Log plot shows the comparison between computed and observed data. Computed data are obtained by introducing the following best fit values into the model:  $K = 200 \text{ m}^2 \text{ s}^{-1}$ ,  $\text{FTT} = 180 \text{ s}$ , and  $\text{PR} = 0.4$ .

[Title Page](#)
[Abstract](#)
[Introduction](#)
[Conclusions](#)
[References](#)
[Tables](#)
[Figures](#)
[◀](#)
[▶](#)
[◀](#)
[▶](#)
[Back](#)
[Close](#)
[Full Screen / Esc](#)
[Printer-friendly Version](#)
[Interactive Discussion](#)


## Tephra hazard assessment at Mt. Etna (Italy)

S. Scollo et al.

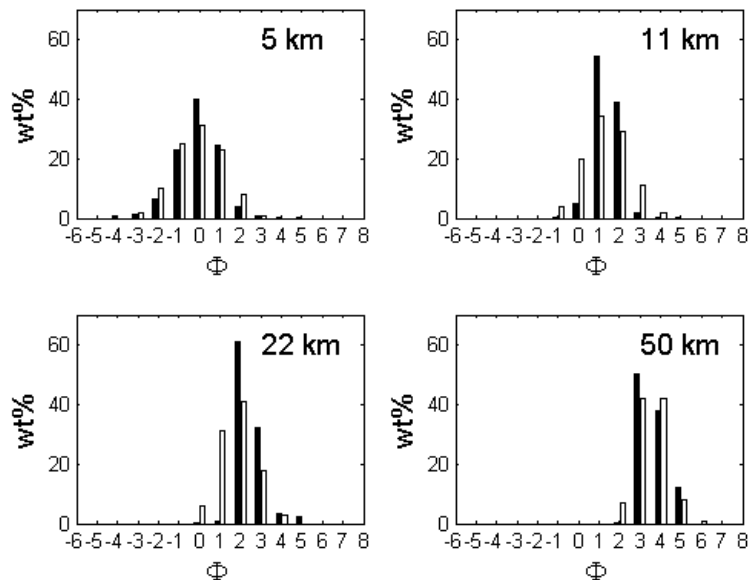


**Fig. 3.** Comparison between observed grain-size distribution of the tephra deposit (black) associated with the 22 July 1998 eruption of Etna (Andronico et al., 1999) and grain-size distribution computed (grey) at the same locations, Rifugio Sapienza, Tardaria, Sant'Agata Li Battiati and Agnone, respectively 5, 11, 22, 50 km from the volcanic vent.

Title Page

Abstract

Introduction

Conclusions

References

Tables

Figures

◀

▶

◀

▶

Back

Close

Full Screen / Esc

Printer-friendly Version

Interactive Discussion



## Tephra hazard assessment at Mt. Etna (Italy)

S. Scollo et al.

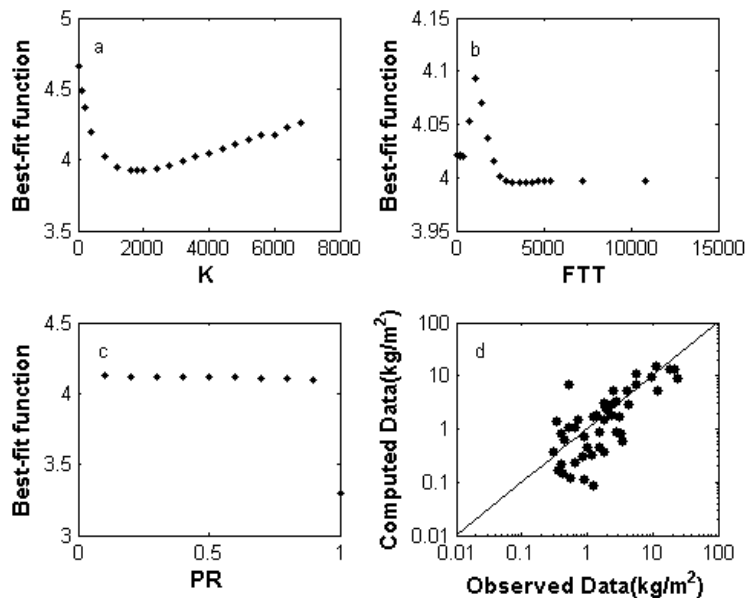


**Fig. 4.** Misfit function calculated varying the atmospheric horizontal diffusion coefficient ( $K$ ) between  $0.001$ – $6800 \text{ m}^2 \text{ s}^{-1}$ , the Fall-Time Threshold (FTT) between  $36$ – $10\,800 \text{ s}$  and PR between  $0$  and  $1$ . Log plot shows the comparison between computed and observed data with the best fit values obtained from the results of sensitivity test for  $K = 1800 \text{ m}^2 \text{ s}^{-1}$ ,  $\text{FTT} = 2520 \text{ s}$  (i.e.  $0.7 \text{ h}$ ) and  $\text{PR} = 1$ .

## Tephra hazard assessment at Mt. Etna (Italy)

S. Scollo et al.

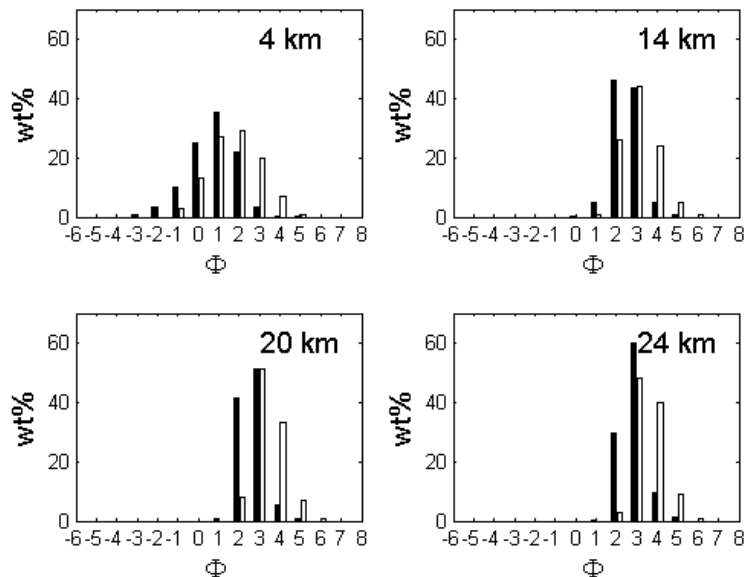


**Fig. 5.** Comparisons between the observed grain-size distribution of the tephra deposit (black) associated with the 21–24 July eruption of Etna and grain-size distribution computed (grey) at the same location. Field data were collected, respectively at about 4, 14, 20, and 24 km from the volcanic vent.

Title Page

Abstract

Introduction

Conclusions

References

Tables

Figures

◀

▶

◀

▶

Back

Close

Full Screen / Esc

Printer-friendly Version

Interactive Discussion



## Tephra hazard assessment at Mt. Etna (Italy)

S. Scollo et al.

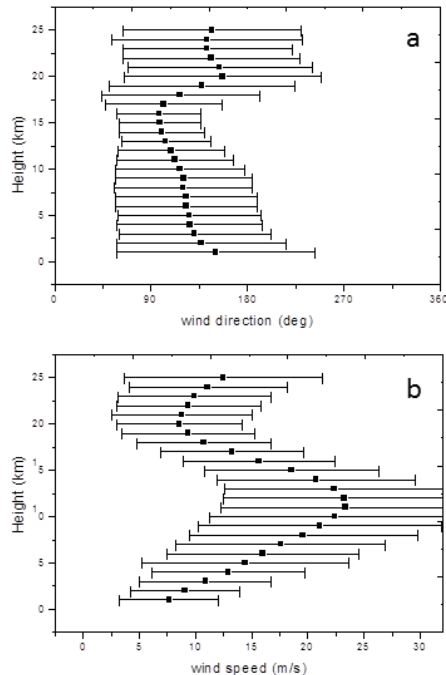


**Fig. 6.** Plots showing: **(a)** the mean wind direction (provenance  $+180^\circ$ ) and **(b)** the mean wind speed every km over 15 yr of wind profiles sampled 4 times a day (00:00; 06:00, 12:00, 18:00 LT) from 1 January 1990 up to 2003. The standard deviation for each height level is also reported. Data are provided by the University of Wyoming and are available at <http://weather.uwyo.edu>.

Title Page

Abstract

Introduction

Conclusions

References

Tables

Figures

◀

▶

◀

▶

Back

Close

Full Screen / Esc

Printer-friendly Version

Interactive Discussion



**Tephra hazard  
assessment at Mt.  
Etna (Italy)**

S. Scollo et al.

Title Page

Abstract

Introduction

Conclusions

References

Tables

Figures

◀

▶

◀

▶

Back

Close

Full Screen / Esc

Printer-friendly Version

Interactive Discussion

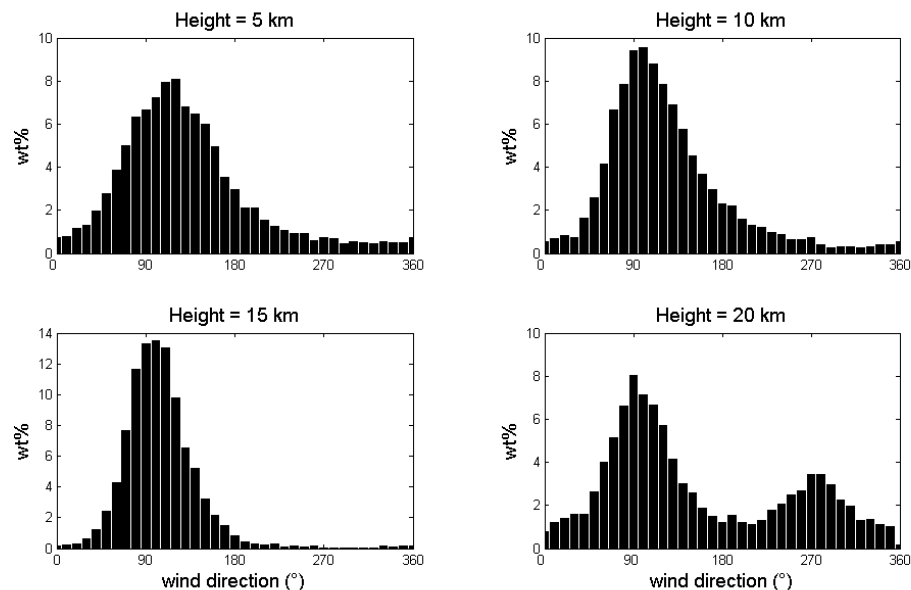


**Fig. 7.** Plots show the percentage of wind direction between 0 and 360° (from the North) at four different altitude level, respectively 5, 10, 15, and 20 km. Data are provided by the University of Wyoming and are available at <http://weather.uwyo.edu>.

## Tephra hazard assessment at Mt. Etna (Italy)

S. Scollo et al.

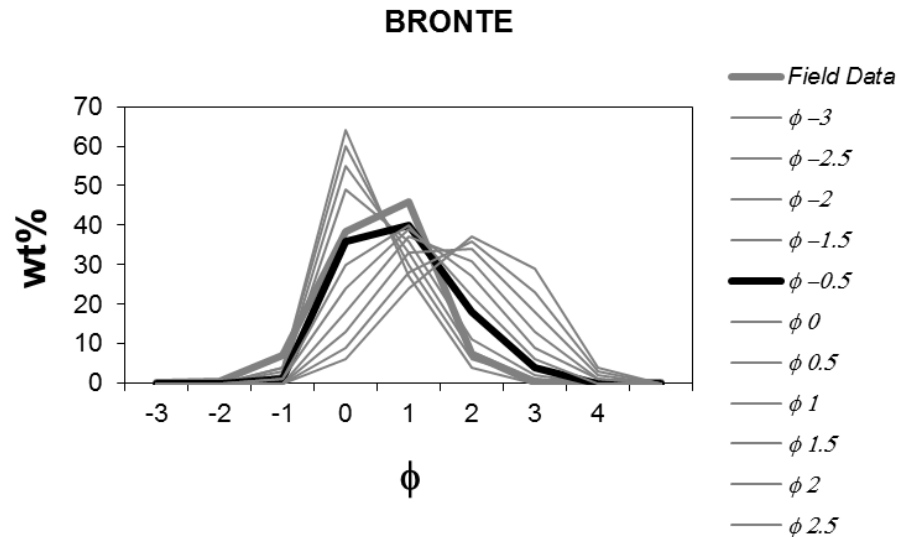


**Fig. 8.** Comparison between the grain-size distribution collected at Bronte (about 15 km from the vent) and computed by TEPHRA at the same locality. The computed total grain-size distribution (TGS) was changed between  $-3$  and  $2.5 \phi$ . The best agreement was obtained for  $-0.5 \phi$ .

Title Page

Abstract

Introduction

Conclusions

References

Tables

Figures

◀

▶

◀

▶

Back

Close

Full Screen / Esc

Printer-friendly Version

Interactive Discussion



## Tephra hazard assessment at Mt. Etna (Italy)

S. Scollo et al.

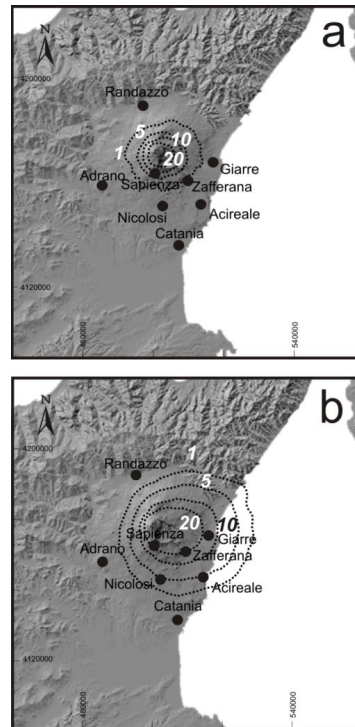


**Fig. 9.** Probability maps for the OES-SSL1 eruption scenario having similar features of 5 January 1990 eruption considering thresholds of **(a)**  $100 \text{ kg m}^{-2}$  and **(b)**  $10 \text{ kg m}^{-2}$ .

Title Page

Abstract

Introduction

Conclusions

References

Tables

Figures

◀

▶

◀

▶

Back

Close

Full Screen / Esc

Printer-friendly Version

Interactive Discussion



## Tephra hazard assessment at Mt. Etna (Italy)

S. Scollo et al.

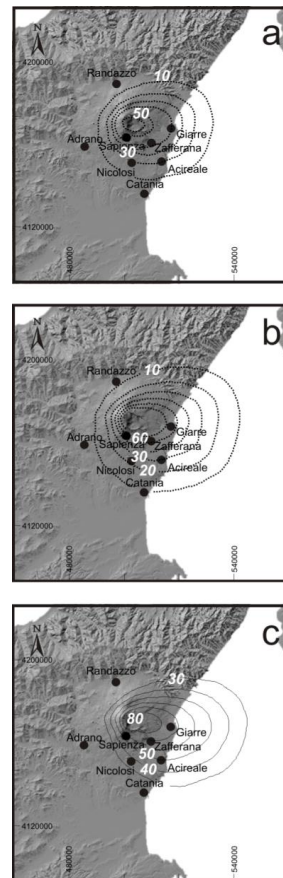


**Fig. 10.** Probability maps for the OES-SSL2 eruption scenario having similar features to the 122BC Plinian eruption considering thresholds of **(a)**  $300 \text{ kg m}^{-2}$ ; **(b)**  $200 \text{ kg m}^{-2}$ , and **(c)**  $100 \text{ kg m}^{-2}$ .

Title Page

Abstract

Introduction

Conclusions

References

Tables

Figures

◀

▶

◀

▶

Back

Close

Full Screen / Esc

Printer-friendly Version

Interactive Discussion



**NHESD**

1, 2945–2981, 2013

**Tephra hazard  
assessment at Mt.  
Etna (Italy)**

S. Scollo et al.

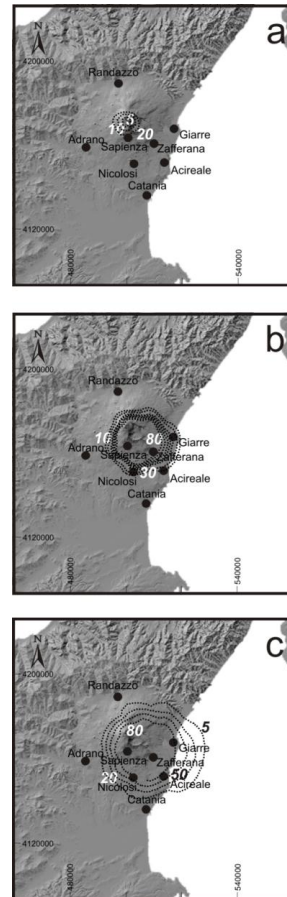


**Fig. 11.** Probability map for the upper limit scenario OES-WLL with similar features to the 2002–2003 eruption. The thresholds shown in figure are **(a)** 300; **(b)** 200, and **(c)** 100  $\text{kg m}^{-2}$ .

Title Page

Abstract

Introduction

Conclusions

References

Tables

Figures

◀

▶

◀

▶

Back

Close

Full Screen / Esc

Printer-friendly Version

Interactive Discussion



**Tephra hazard  
assessment at Mt.  
Etna (Italy)**

S. Scollo et al.

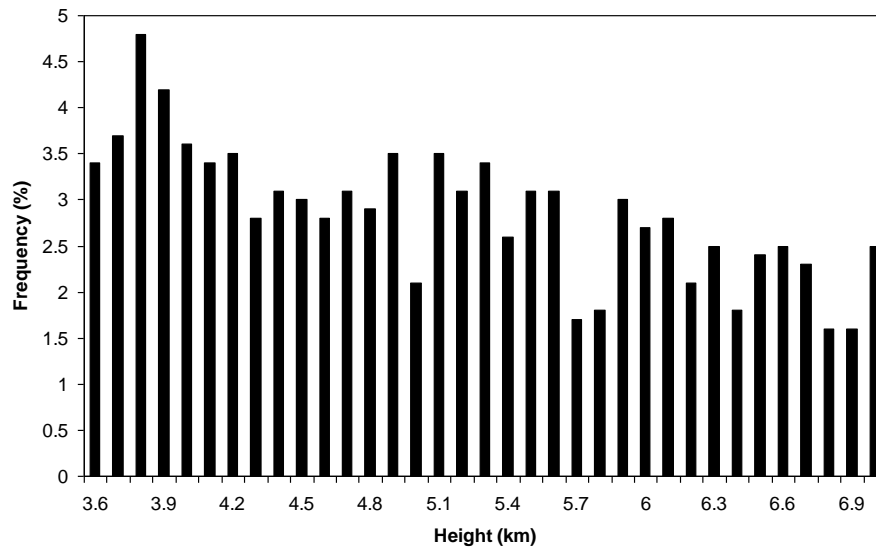


**Fig. 12.** Frequency of sampling of the column height in the Eruption Range Scenario (ERS-WLL).

[Title Page](#)[Abstract](#)[Introduction](#)[Conclusions](#)[References](#)[Tables](#)[Figures](#)[◀](#)[▶](#)[◀](#)[▶](#)[Back](#)[Close](#)[Full Screen / Esc](#)[Printer-friendly Version](#)[Interactive Discussion](#)

## Tephra hazard assessment at Mt. Etna (Italy)

S. Scollo et al.

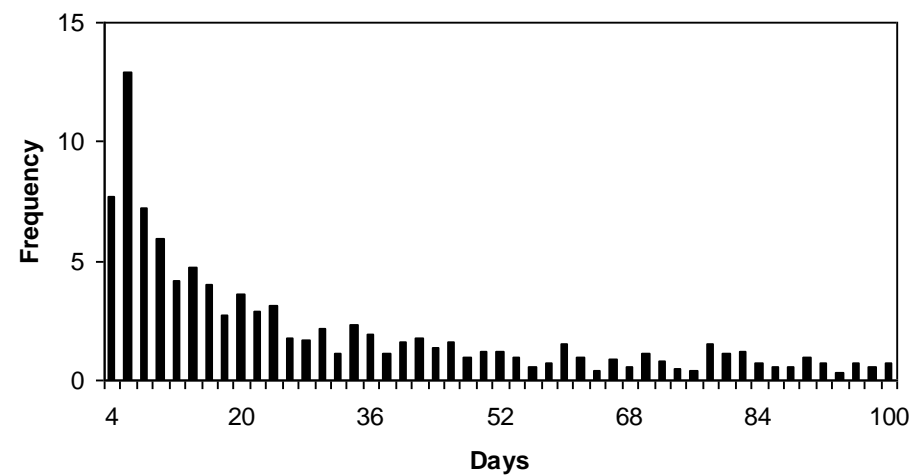


**Fig. 13.** Frequency of sampling (days) in the Eruption Range Scenario (ERS-WLL).

Title Page

Abstract

Introduction

Conclusions

References

Tables

Figures

◀

▶

◀

▶

Back

Close

Full Screen / Esc

Printer-friendly Version

Interactive Discussion



## Tephra hazard assessment at Mt. Etna (Italy)

S. Scollo et al.

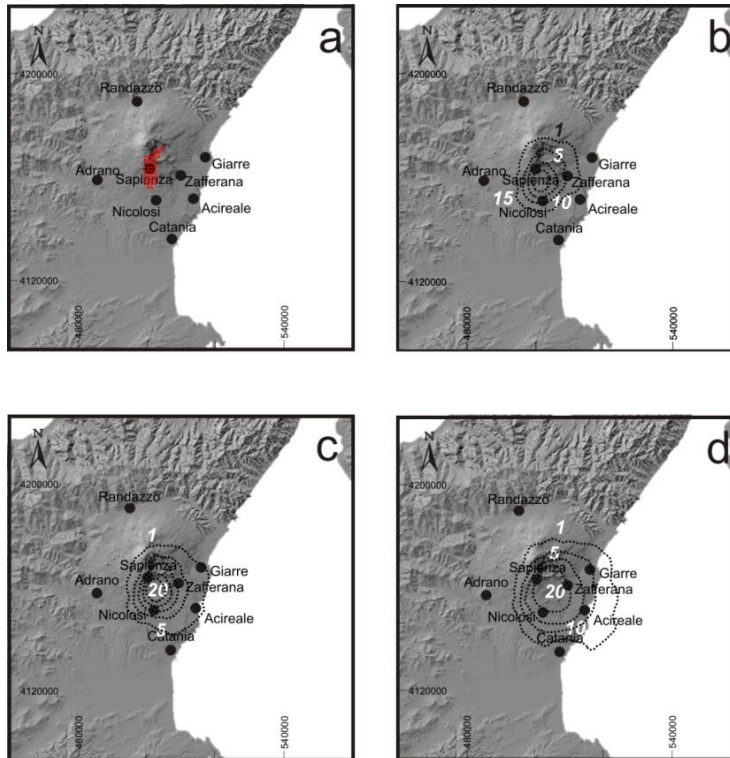


**Fig. 14.** (a) Location of volcanic vents sampled statistically in ERS-WLL. Probability maps for the eruption range scenario of ERS-WLL using the thresholds: (b) 300; (c) 200, and (d)  $100 \text{ kg m}^{-2}$ .

Title Page

Abstract

Introduction

Conclusions

References

Tables

Figures

◀

▶

◀

▶

Back

Close

Full Screen / Esc

Printer-friendly Version

Interactive Discussion

